Solar cycle variation of ion outflow observed by Akebono/SMS

Manabu Yamada, and Shigeto Watanabe

Department of Earth and Planetary Sciences, Hokkaido University Kita-ku, Sapporo, Japan

Takumi Abe

Institute of Space and Astronautical Science, Sagamihara, Japan

Eiichi Sagawa

Communication Research Laboratory, Koganei, Japan

A. W. Yau

Institute of Space Research, University of Calgary, Canada

Short title:

Abstract. The Suprathermal ion Mass Spectrometer (SMS) onboard EXOS–D (Akebono) satellite has measured low energy ($<$ 25 eV) ion energy distribution in the polar ionosphere from 1989. We constructed a database on plasma parameters such as velocity, density, temperature, and flux of H^+, He^+, and O^+based on SMS data in the period of 1989-2000. The database includes also solar flux and geomagnetic index. We investigated statistically the distribution of polar ion outflow for altitude, invariant latitude, magnetic local time, and the solar and geomagnetic activities. The ion outflow with velocity over 2 km/sec occurs frequently in the region of topside polar ionosphere near Auroral and polar cap boundary regions (invariant latitude $>$ 60 degrees, altitude $>$ 6000 km). The ion outflow comes from both polar wind and low energy ion conics ($<$ 20eV) heated perpendicular to local magnetic field line in the cusp and near the aurora region. During the geomagnetic disturbance, the region occurring large ion flux shifts to low latitude region. The flux was also dependent upon the solar activity. **At km altitude**, the fluxes of H^+, He^+, and O^+were $\sim 10^{11}$ ions $m^{-2}s^{-1}$, $\sim 10^{11}$ ions $m^{-2}s^{-1}$, $\sim 10^{10}$ ions $m^{-2}s^{-1}$during the solar maximum in 1990–1991 and $\sim 10^{10}$ ions $m^{-2}s^{-1}$, $\sim 10^{9}$ ions $m^{-2}s^{-1}$, $\sim 10^{9}$ ions $m^{-2}s^{-1}$near the solar minimum condition in 1993–1994, respectively. For all ion species, the flux decreased with decrease of solar activity but the flux increased again during the solar minimum. We suggest that neutral hydrogen density increased at altitudes of ion heating region in the solar minimum condition and $H^+$was produced by a charge exchange reaction in the region of polar topside ionosphere. The ion velocity increased during the solar minimum. The drift energy may come from low collision frequency between ion and neutral particles in the low solar activity condition or the enhancement of wave activity accerelating the ions.

1. Introduction

Ion outflow from topside polar ionosphere is important as a loss of atmosphere and a source of magnetospheric plasma. Young et al. [1982] showed that the magnetospheric plasma density such as $H^+$and $O^+$are correlated with both Kp index and solar EUV flux. Particularly the density was associated with increase of EUV flux during the rising phase of solar cycle. They suggested that the $H^+$and O^+observed in the magnetosphere were resulted in the high latitude ionosphere.

Light ion ($H^+$and O^+) escape from topside polar ionosphere along a geomagnetic field line was studied as an evaporative process of thermal ions [Bauer, 1966; Dessler and Michel, 1966]. Banks and Holzer [1968] and Axford [1968] suggested that the ion outflow with supersonic speed was possible in the open magnetic field line and O^+flow must be negligibly small compared to H^+. The flow is referred as ”polar wind”.

The first direct observation of the polar wind was made on Explorer 31 and ISIS 2 satellites [Brinton et al., 1971; Hoffman et al., 1974]. Dynamics Explorer 1 (DE-1) found the frequent outflow of hot $H^+$and O^+over the polar cap [Shelley et al., 1982, Chappell et al., 1982, Gurgiolo and Burch, 1982]. Gurgiolo and Burch [1982] interpreted the ion with energy of 10 - 100 eV as the polar wind heated perpendicularly to local magnetic field line at lower altitudes. After that, ion outflows including O^+have been confirmed by various observations by radar [Wu et al., 1992], rockets [Arnoldy et al., 1996] and satellites [Abe et al., 1993; Norqvist et al., 1998; Lund et al., 1999]. Those observations showed that nonthermal ion heating forming ion beam and ion conic is important process of ion outflow in the polar topside ionosphere.

To investigate the spatial and temporal distribution of ion outflow phenomena in the polar topside ionosphere and its dependence on geomagnetic and solar activities, statistical analyses based on long-term observation are needed. The early studies based on the data of S3-3 and DE-1 showed the occurrence frequency of ion outflow at altitudes of 1000 – 8000 km and 8000 – 23000 km, respectively. From the ion composition data on S3-3, Ghielmetti et al. [1978] showed that there was some relationship between statistical Auroral oval and the region where ion outflow phenomena with energy range from 0.5 keV to 16 keV occurred. Gorney et al. [1981] analyzed the electrostatic analyzer data on S3-3 and concluded that ion beam and conic were common phenomenon in Aurora region. The occurrence frequencies of ion beam and conic in latitude, local time and altitude showed the dependence on geomagnetic activity. The data from the energetic ion composition spectrometer (EICS) on DE-1 provided us information on ion outflow [Yau et al., 1984; Kondo et al., 1990]. The occurrence frequency was dependent upon solar activity as well as geomagnetic activities [Yau et al., 1985a, 1985b]. From 100000 data obtained by DE-1, Yau et al. [1985a] showed also the variation of occurrence frequency of ion outflow in the declining phase of solar cycle 21 from 1981 to 1984. They indicated that the occurrence of O^+outflow was higher in the solar maximum condition than that in the solar minimum condition.

2. Construction of thermal ion database

Akebono satellite, which was launched on February 1989 in elliptic orbit with an apogee of $\sim$10000 km, a perigee of 270 km, an inclination of 75 $^\circ$. and an orbital period of 212 minutes, has observed Aurora and its related phenomena over 10 years. The suprathermal Ion Mass Spectrometer (SMS) on Akebono measures ion energy distribution function of $f(\mathrm{E})$ with the energy from 0 to 25 eV in the satellite spin plane for every one spin period of 8 seconds [Whalen et al., 1990]. From large amount of data obtained by the SMS, we constructed a database which includes plasma parameters such as parallel velocity, density, temperature and flux for H^+, $He^+$and O^+, satellite position, $K_p$index and $F_{10.7}$. Watanabe et al. [1992] established a calculation algorithm of plasma parameter based on the SMS data. By the use of the method, ion density N, ion velocity V_0, temperature T_0 and satellite potential are estimated in the satellite spin plane from calculations of moment of the ion energy distribution function. We have modified their method to calculate plasma parameters in three dimensional velocity space, where we assume that ion energy distribution function f_i is symmetry to a local magnetic field line by cyclotron motion. The following integrals for each ion species are, therefore, used in our present study:

$$N = \int f_i(V,\phi) V dV d\phi d\theta \quad (1)$$

$$V_{0\|} = \frac{1}{N} \int \mathbf{V} \cdot (\mathbf{s} \times \mathbf{t}) f_i(V,\phi) dV d\phi d\theta \quad (2)$$

$$V_{0\perp} = \quad (3)$$

$$T_0 = \frac{m_i}{2kN} \int (\mathbf{V} - \mathbf{V}_0)^2 f_i(V,\phi) dV d\phi d\theta \quad (4)$$

where $\mathbf{s}$ is a unit vector in spin axis direction, $\mathbf{t}$ is a unit vector perpendicular to both $\mathbf{s}$ and local magnetic field, k is the Boltzmann constant, m_i is ion mass, V, ϕ and θ are the velocity in the spin plane, pitch angle from direction of local magnetic field line and azimuth angle, respectively. **Since the ion energy distribution function is measured in the satellite**

spin plane, the ion density is lower than the real density when the ion has the velocity component perpendicular to the satellite spin axis. The angle between the spin plane and the magnetic field line is less than 30 $^\circ$ in the polar region because the spin axis directs to the sun. The angle arises the accuracy of ion density calculations. Ion drift by polar cup convection or satellite velocity component to the spin axis is $\sim$ 2km/s or less at mid altitude of topside ionosphere in the polar cup region. Since the velocity is smaller than the local ion thermal velocity, the accuracy of density or flux estimations is lower than a factor of 2. The velocity and temperature do not have such effect but they may have some error if the ion energy distribution function would have different high energy component such as high energy tail.

Figure 1 shows an example of ion energy distribution obtained by SMS near the northern cusp on February 20, 1990 and plasma parameters calculated with equations (1)-(3). Figure 1 (a)-(c) show color-coded energy/spin angle spectrograms of H^+, $He^+$and O^+as functions of universal time (UT), altitude (ALT), magnetic latitude (MLAT) and magnetic local time (MLT). The energy range is from 0 to 25 eV. Spin angle of 0 degree in the spin plane corresponds to the minimum pitch angle For all ion spe to the local magnetic field line. Ion flow at 0 degree means downward flow in the northern hemisphere. Figure 1 (d)-(f) show drift velocity, $V_\perp$ (km/s), perpendicular to magnetic field line, field-aligned velocity, $V_{||}$ (km/s), and ion temperature, T (K), calculated with equations (1)–(4). Characters of ’H’, ’4’ and ’O’ represent H^+, $He^+$and O^+, respectively. Positive perpendicular and parallel velocities means eastward and upward flows. Transverse ion energization occurred through cusp region in 1638 – 1643 UT for all ion species. Ion upward velocities and temperatures around the cusp increase in comparison with the value at low latitude. Ion outflow like a polar wind occurred in the polar cap region ($>$ 1655 UT). (T_i **について Drakou et al を参照**)

Figure 2 shows another example obtained in nightside auroral region on March 16, 1993. The display format is same to figure 1. The satellite was in the auroral electron precipitation region in the period of 1735 – 1814 UT and all ions flew upward with both high velocity and temperature. We have constructed a database with $\sim$370,000 data sets covered the time period from February 1989 through 2000.

We used the database to reveal the characteristics of ion outflow phenomena occurred in the polar topside ionosphere.

3. Characteristic of ion outflow

3.1. Altitude distribution of ion velocity and flux

Figure 3 shows altitude distribution of H^+,$He^+$and O^+velocities (km/sec) parallel to magnetic field line in the invariant latitude larger than 75 $^\circ$. Red and green dots represent the velocity measured in northern and southern hemispheres, respectively. Positive velocity means upward flow from ionosphere to magnetosphere. The velocities in both hemispheres increase with increasing of altitude and reach $\sim$10 km/s for H^+, $\sim$6 km/s for $He^+$and $\sim$3 km/s for O^+at $\sim$10000 km altitude. Altitude distribution of H^+, $He^+$and O^+fluxes ($\log{(\mathrm{m}^{-2}\mathrm{s}^{-1})}$) parallel to magnetic field line in the polar cap region is shown in Figure 4. Since both production and loss rates are negligible in the topside ionosphere, ion flux ,F, must be conserved in the steady state condition as

$$FA = \text{constant} \tag{5}$$

where F represents ion density (N) times ion bulk velocity (V) which are measured by SMS and A is cross section of a local magnetic field ($\mathbf{B}$). Cross section, A, is written as $A \propto R^3$ where R is a distance from center of the earth, Then equation (5) is rewritten to following:

$$F = \frac{F_0 R_0^3}{R^3} \tag{6}$$

where $R_0^3 F_0$ represents reference flux as which we used averaged fluxes of 9000 - 10000 km. The fluxes are 2.1×10^{10} ions $m^{-2}s^{-1}$for H^+, 3.4×10^9 ions $m^{-2}s^{-1}$for $He^+$and 1.0×10^{10} dens for O^+. In figure 4, blue line shows average upward flux and black line is the flux calculated by equation (5). We note that the calculated lines agree with the measured upward flux. It means that the ion flux is conserved along a magnetic field line in the topside ionosphere.

As shown in figure 3. the different ion species have significant upward velocities. The velocity increase with increasing of altitude indicates that there is the continual acceleration below 10000 km altitude for both light and heavy ions. It agrees with the results of Chandler et al. (1991) and Abe et al. (1993). However, theoretical works predict significant outflow of $H^+$and He^+but negligible outflow of O^+due to the large gravitational force (Banks and Holzer, 1968) and charge exchange of $O^+$with neutral hydrogen (Banks et al., 1974; Raitt et al., 1975). Satellite observations showed clearly the energetic O^+outflow from the polar ionosphere due to ion heating (Ghielmetti et al., 1978; Collin et al 1981; Shelley et al., 1982; Yau et al., 1984, 1985a; Waite et al., 1985; Moore et al., 1986; Lund et al., 2000). (**1keV の観測,sms のは $\sim$10eV**) We suggest that acceleration of heavy ions observed by Akebono/SMS come from ion heating and conics (see figure 1 and 2; Yoshida et al. 2000), and the flux is approximately constant in the topside polar ionosphere.

3.2. Dependence on geomagnetic activity

Figure 5 shows H^+, $He^+$and O^+upward velocities in invariant latitude – magnetic local time space in the northern hemisphere for different magnetic activities. We used the data at 6000 – 9000 km altitudes in 1989 – 1998. Figure 5 (a), (d) and (g) show H^+, $He^+$and O^+velocity distribution in the low geomagnetic activity condition ($K_p < 2^+$), respectively. Color bar represents a magnitude of upward velocity (km/sec). We note that ions flow upward everywhere in the polar region (invariant latitude $>$ 60 deg), and ions with high velocity occur near auroral oval and in the poleward region of averaged auroral oval. Figure 5 (b), (e), (h) and (c), (f), (i) show H^+, $He^+$and O^+velocity distribution in middle ($3^- \geq K_p \geq 4^+$) and high ($5^- \geq K_p$) geomagnetic activity conditions, respectively. The region occurring large flow shifts to low latitude during geomagnetic disturbance.

Abe et al. (1993) carried out similar analyses by use of SMS data obtained in the period of 1990 – 1991. However, they showed the distribution during the solar minimum Yau et al. (1984) showed invariant latitude – local time distribution of the occurrence frequencies for both $H^+$and O^+outflow with 0.01 - 1 keV with DE-1 data. Our result shown in figure 5 is consistent with Yau et al. (1984). However, we point out that average ion velocity is positive in the polar topside ionosphere. It means that polar ion flows outward anytime in the polar region. We suggest also that high velocity occurring near Aurora region results in mainly ion heating and conics as shown in figures 1 and 2. Yau et al. (1985b) and Kondo et al. (1990)

showed that both the occurrence frequency and the averaged flux increase with increasing geomagnetic activity. From Vikinig ion data, Oieroset et al. (1999) showed ion flux resulted in ion beams and conics observed in the dayside ionosphere and obtained a strong increase of the occurrence in the cusp region during substorm. The flux and the dependence on magnetic activity agree with our statistical study.

3.3. Solar cycle variation

Figure 6 shows H^+, $He^+$and O^+upward fluxes averaged by every 45 days at 5000 – 10000 km altitudes in invariant latitude lager than 60 °during 10 years. $F_{10.7}$ is also plotted in the bottom of figure 6. Red and Green dots in the top three panels represent fluxes estimated in northern and southern hemispheres, respectively. Periodic variations of ion fluxes with ∼9 months (270 days) are due to the satellite altitude variations; apogee changes from one hemisphere to another hemisphere for ∼9 months. The fluxes of H^+, $He^+$and $O^+$are $\sim 10^{11}$ ions $m^{-2}s^{-1}$, $\sim 10^{10}$ ions $m^{-2}s^{-1}$and $\sim 10^{10}$ ions $m^{-2}s^{-1}$during the solar maximum in 1990 – 1991. Ion flux measured in 1993 – 1994 was one order less than that in 1990 – 1991. The flux decreases with decrease of solar activity but the flux increases again during the solar minimum.

As shown in figure 7 and 8, ion flux variation is mainly due to ion density variation while the averaged ion velocity at 5000–9000km altitudes is approximately constant during 10 years. However, ion velocity increases slightly during the solar minimum (see figure 8). It is due to that collisions between ions and ions and between ions and neutral particles control ion flow velocity in the polar topside ionosphere. If collision frequency of ions would be large in the high solar activity condition, it is difficult for ions to be accelerated in the topside ionosphere. The another accerelation mechanism is low energy ion conics generated by low frequency waves. The waves may be important acceretion source in the topside ionosphere (Kasahara et al., 2001).

Density ratios between different ion species are shown in figure 9. We note that both H^+/$O^+$and H^+/He^+density ratios increase in the low solar activity but He^+/O^+ratio dose not change largely during 10 years. It shows that neutral hydrogen density increases in ion heating/acceleration region in the low solar activity and $H^+$is produced by a charge exchange reaction as

$$H^+ + O \rightleftharpoons H + O^+ \tag{7}$$

in the region of polar topside ionosphere.

4. Summary

The Suprathermal ion Mass Spectrometer (SMS) on Akebono satellite measures low energy (< 25 eV) ion energy distribution in the satellite spin plane. We have calculated plasma parameters of velocity, density and temperature for H^+, $He^+$and $O^+$and satellite potential to the ambient plasma from SMS data in the period of 1989 – 2000. We investigated the dependency between the parameters and solar and geomagnetic activities.

From our statistical analyses, we summarize the following;

1. H^+, $He^+$and O^+ions flow upward in polar region (invariant latitude $>$ 60 degrees) with velocity of $\sim$10 km/s, $\sim$6 km/s and $\sim$3 km/s near 10000 km altitude.

2. Region with high velocity occurs near the Aurora region and in the poleward of averaged Aurora oval. Ion velocity is high near the cusp region. Ions with high velocity are mainly associated with the ion heating and conics.

3. The region with high velocity shifts to low latitude during the geomagnetic disturbance. The heating region near cusp shifts from invariant latitude of 78 degrees ($K_p < 2^+$) to that of 75 degrees ($K_p > 5^+$).

4. Upward ion flux is conserved along a magnetic field line in the topside ionosphere. The flux was dependent upon the solar activity. The fluxes of H^+, He^+, and O^+were $\sim 10^{11}$ ions $m^{-2}s^{-1}$, $\sim 10^{10}$ ions $m^{-2}s^{-1}$, $\sim 10^{10}$ ions $m^{-2}s^{-1}$, during the solar maximum in 1990-1991 and $\sim 10^{10}$ ions $m^{-2}s^{-1}$, $\sim 10^{9}$ ions $m^{-2}s^{-1}$, $\sim 10^{9}$ ions $m^{-2}s^{-1}$, near the solar minimum condition in 1993-1994, respectively.

5. The flux decreases with decrease of solar activity but the flux increases again during the solar minimum. It suggests that neutral hydrogen density increases in ion heating/acceleration region in the low solar activity and $H^+$is produced by a charge exchange reaction in the region of polar topside ionosphere.

6. Ion velocity increases slightly during the solar minimum. It indicates that collision frequency between ion and neutral particles is low in the low solar activity condition.

The ion acceleration mechanism is the subject of detailed analyses of an extensive data set of thermal ions, energetic electron and ion and waves from Akebono satellite. This study is currently in progress.

Acknowledgments. The EXOS-D SMS instrument development was supported by the Canadian Space Agendy. We wish to acknowledge the valuable cooperation and assistance from members of the EXOS-D science team.

References

Abe, T., M. A. Whalen, A. W. Yau, R. E. Horita, S. Watanabe, and E. Sagawa, EXOS–D (Akebono) SMS observation of the polar wind, J. Geophys. Res., 98, 11191-11203, 1993.

Arnoldy, R. L., K. A. Lynch, P. M. Kintner, J. Bonnell, T. E. Moore, and C. J. Pollock, SCIFIER – structure of the cleft ion fountain at 1400 km altitude, Geophys. Res. Lett., 23, 1869-1872, 1996.

Axford, W. I., The polar wind and the terrestrial heilium budget, J. Geophys. Res., 73, 6855–6859, 1968.

Banks, P. M., and T. E. Holzer, The plolar wind, J. Geophys. Res., 73, 6846–6854, 1968.

Banks, P. M., R.W. Schunk and W.J. Raitt, Temperature and density structure of thermal proton flows, J. Geophys. Res., 79, 4691–4702, 1974.

Bauer, S. J, The structure of the topside ionosphere, in Electron Density Profiles in Ionosphere and Exosphere, edited by J. Frihagen, p. 387, North–Holland, Amsterdam, 1966.

Brinton, H. C., J. M. Grebowsky, and H. G. Mayr, Altitude variation of ion composition in the mid–latitude trough region: Evidence for upward plasma flow, J. Geophys. Res., 76, 3738–3745, 1971.

Chandler, M.O., J.H. Waite, Jr., T.E. Moore, Observations of polar ion outflows, J. Geophys. Res., 96, 1421–1428, 1991.

Chappell, C. R., J. L. Green, J. F. E. Johnson, and J. H. Waite, Jr., Pitch angle variations in magnetospheric thermal plasma — Initial observations from Dynamics Esplorer–1, Geophys. Res. Lett., 9, 933–936 ,1982.

Collin, H.L., R.D. Sharp, E.G. Shelly, and R.D. Johnson, Some general characteristics of upflowing ion beams over the auroral zone and their relationship to auroral electrons, J. Geophys. Res., 86, 6820–6826, 1981.

Dessler, A. J., and F. C. Michel, Plasma in the geomagnetic tail, J. Geophys. Res., 71, 1421–1426, 1966.

Ghielmetti, A. G., R. G. Johnson, R. D. Sharp, and E. G. Shelley, The latitudinal, diurnal, and altitudinal distributions of upward flowing energetic ions of ionospheric origin, Geophys. Res. Lett., 5, 59–62, 1978.

Gorney, D. J., A. Clarke, Croley, J. Fennell, J. Luhmann, and P. Mizera, The Distribution of Ion Beams and Conics Below 8000 km, J. Geophys. Res., 86, 83–89, 1981.

Gurgiolo, C., and J. L. Burch, DE–1 observations of the polar wind — A heated and unheated component, Geophys. Res. Lett., 9, 945–948, 1982.

Hoffman, J. H., W. H. Dodson, C. R. Lippincott, and H. D. Hammack, Initial ion composition results from the ISIS satellite, J. Geophys. Res., 79, 4246–4251, 1974.

Kondo, T., B. A. Whalen, and A. W. Yau, Statistical Analysis of Upflowing Ion Beam and Conic Distributions at DE 1 Altitudes, J. Geophys. Res., 95, 12,091–12,102, 1990.

Lund, E.J., E. Mobius, C.W. Carlson, R.E. Ergun, L.M. Kistler, B. Klecker, D.M. Klumpar, J.P. McFadden, M.A. Popecki, R.J. Strangeway, and Y.K. Tung, Transverse ion acceleration mechanisms in the aurora at solar minimum: occurrence distributions, J. Atmos. Solar–Terr. Phys., 62, 467–475, 2000.

Lundin, R., L. Eliasson, B. Hultqvist, and K. Stasiewicz, Plasma energization on auroral field lines as observed by the Viking spacecraft, Geophys. Res. Lett., 14, 443–446 ,1987.

Norqvist, P., M. André, and M. Tyrland, A statistical study of ion energization mechanisms in the auroral region, J. Geophys. Res., 103, 23,459–23,473, 1998.

Moore, T.E., M. Lockwood, M.O. Chandler, J.H. Waite, Jr., C.R. Chappell, A.M. Persoon and M.

Sugiura, Upwelling O^+ion source characteristics, J. Geophys. Res., 91, 7019–7031, 1986.

Oieroset, M., M. Yamauchi, L. Liszka, S.P. Christon, and B. Hultqvist, A statistical study of ion beams and conics from the dayside ionosphere during different phases of a substorm, J. Geophys. Res., 104, 6987-6998, 1999.

Raitt, W.J., R.W. Schunk and P.M. Banks, A comparison of the temperature and density structure in high and low speed thermal proton flows, Planet. Space. Sci., 23, 1103–1117, 1975.

Shelley, E. G., W. K. Peterson, A. G. Ghielmetti, and J. Geiss, The polar ionosphere as a source of energetic magnetospheric plasma, Geophys. Res. Lett., 9, 941-944, 1982.

Waite, J.H., Jr., T. Nagai, J.F.E. Johnson, C.R. Chappell, J.L. Burch, T.L. Killeen, P.B. Hays, G.R. Corignan, W.K. Peterson, and E.G. Shelly, Escape of suprathermal O^+ions in the polar cap, J. Geophys. Res., 90, 1619–1630, 1985.

Watanabe, S., M. A. Whalen, and A. W. Yau, Thermal ion obserbations of depletion and refilling in the plasmaspheric trough, J. Geophys. Res., 97, 1081–1096, 1992.

Whalen, B.A., J. R. Burrows, A. W. Yau, E. E. Budzinski, A. M. Pilon, I. Iwamoto, K. Marubashi, S. Watanabe, H. Mori, and E. Sagawa, The Suprathermal Ion Mass Spectrometer (SMS) for the Akebono (EXOS-D) spacecraft, J. Geomag. Geoelectr., 42, 511-536, 1990.

Wu, J., M. Blanc, D. Alcaydé, A. Barakat, J. Fontanari, P.-L. Blelly, and W. Kofman, Observations of the structure and vertical transport of the polar upper ionosphere with the EISCAT VHF radar: 2. First investigations of the topside $O^+$and H^+vertical ion flows, Ann. Geophysicae, 10, 375-393, 1992.

Yau, A. W., B. A. Whalen, W. K. Peterson and E. G. Shelley, Distribution of Upflowing Ionospheric Ions in the High–Altitude Polar Cap and Auroral Ionosphere, J. Geophys. Res., 89, 5507-5522, 1984.

Yau, A. W., P. H. Beckwith, W. K. Peterson and E. G. Shelley, Long-Term (Solar Cycle) and Seasonal Variations of Upflowing Ionospheric Ion Events at DE 1 Altitudes, J. Geophys. Res., 90, 6395-6407, 1985a.

Yau, A. W., E. G. Shelley, W. K. Peterson, and L. Lenchyshyn, Energetic auroral and polar ion outflow at DE 1 altitudes: Magnitude, composition, magnetic activity dependence, and long-term vatiations, J. Geophys. Res. 90, 8417-8432,1985b.

Yoshida, N., S. Watanabe, H. Fukunishi, T. Sakanoi, T. Abe, T. Mukai, H. Hayakawa, A. Matsuoka, Y. Kasahara, R. Fujii, S. Nozawa, Y. Ogawa, M. Syrjasuo, Coordinated Akebono and EISCAT observations of suprathermal ion outflows in the nightside inverted-V region, in print, J. Atmos. Solar-Terr. Phys., 62, 449-465, 2000.

Young, D. T., H. Balsiger, and J. Geiss, Correlations of Magnetospheric Ion Composition With Geomagnetic and Solar Activity, J. Geophys. Res. 87, 9077-9096, 1982.

Received ________________________

Figure 1: An example of ion energy distribution obtained by SMS near the northern cusp on February 20, 1990 and the estimated plasma parameters. Panel (a)-(c) show color-coded energy/spin angle spectrograms of H^+, $He^+$and O^+as functions of universal time (UT), altitude (ALT), magnetic latitude (MLAT) and magnetic local time (MLT). The energy range is from 0 to 25 eV. Spin angle of 0 degree in the spin plane corresponds the minimum pitch angle to the local magnetic field line. Panel (d)-(f) show drift velocity, $V_\perp$ (km/s), perpendicular to magnetic field line, field-aligned velocity, $V_\parallel$ (km/s), and ion temperature, T (K). Characters of 'H', '4' and 'O' represent H^+, $He^+$and O^+, respectively. Positive parallel velocity means upward flow.

Figure 2: SMS data obtained in nightside Aurora region on March 16, 1993 and the estimated plasma parameters. The satellite was in the Aurora electron precipitation region in the period of 1735 – 1814 UT and all ions flow upward with both high velocities and temperatures.

Figure 3: Field aligned velocities for H+, He+ and O+ in the invariant latitude larger than 75 degrees. Red and green dots represent the velocity measured in northern and southern hemispheres, respectively. Positive velocity means upward flow from ionosphere to magnetosphere.

Figure 4: Field aligned fluxes for H^+, $He^+$and O^+in the invariant latitude larger than 75 degrees. Blue line shows average upward flux and black line is the calculated flux with equation (5).

Figure 5: H^+, $He^+$and O^+upward velocities in invariant latitude – magnetic local time space in the northern hemisphere for different magnetic activities. The data at 6000 – 9000 km altitudes in 1989 – 1998 are used. The region occurring large flow shifts to low latitude during

geomagnetic disturbance.

Figure 6: H^+, $He^+$and O^+upward fluxes at 5000 – 10000 km altitudes in invariant latitude lager than 60 deg during 10 years. Sunspot numbers are also plotted in the bottom of figure. Red and Green dots in the top three panels represent fluxes estimated in northern and southern hemispheres, respectively.

Figure 7: H^+, $He^+$and O^+densities at 5000 – 10000 km altitudes in invariant latitude lager than 60 deg during 10 years.

Figure 8: H^+, $He^+$and O^+velocities at 5000 – 10000 km altitudes in invariant latitude lager than 60 deg during 10 years. Ion velocity is approximately constant during 10 years but the velocities increase slightly during the solar minimum.

Figure 9: Density ratios between different ion species are shown in figure 9. Both $H^+/O^+$and H^+/He^+density ratios increase in the low solar activity but He^+/O^+ratio dose not change largely during 10 years.

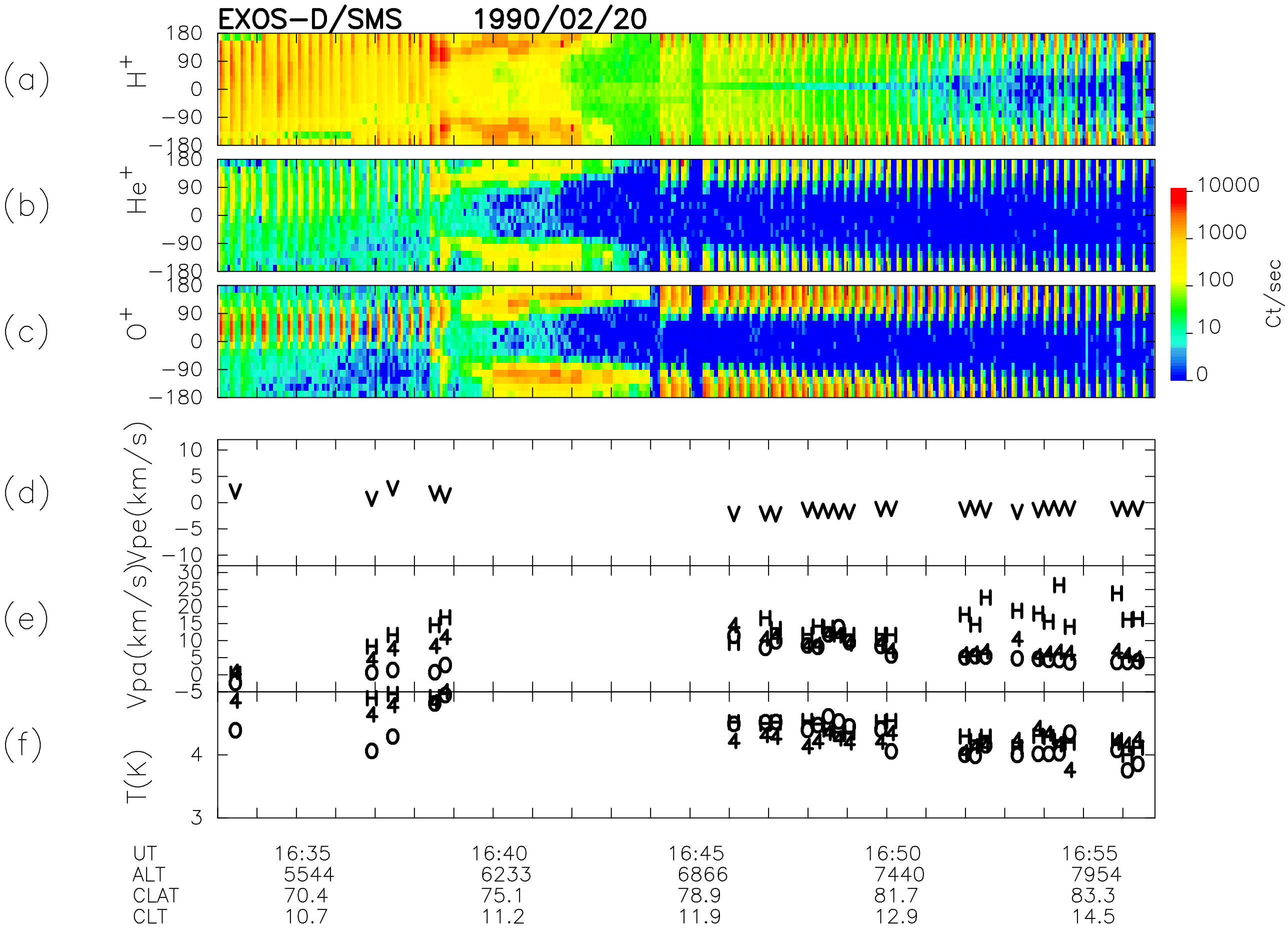
EXOS-D/SMS 1990/02/20
(a)
H+
(b)
He+
(c)
O+
(d)
Vpe(km/s)
(e)
Vpa(km/s)
(f)
T(K)
Ct/sec
10000
1000
100
10
0
UT 16:35 16:40 16:45 16:50 16:55
ALT 5544 6233 6866 7440 7954
CLAT 70.4 75.1 78.9 81.7 83.3
CLT 10.7 11.2 11.9 12.9 14.5

Figure 1.

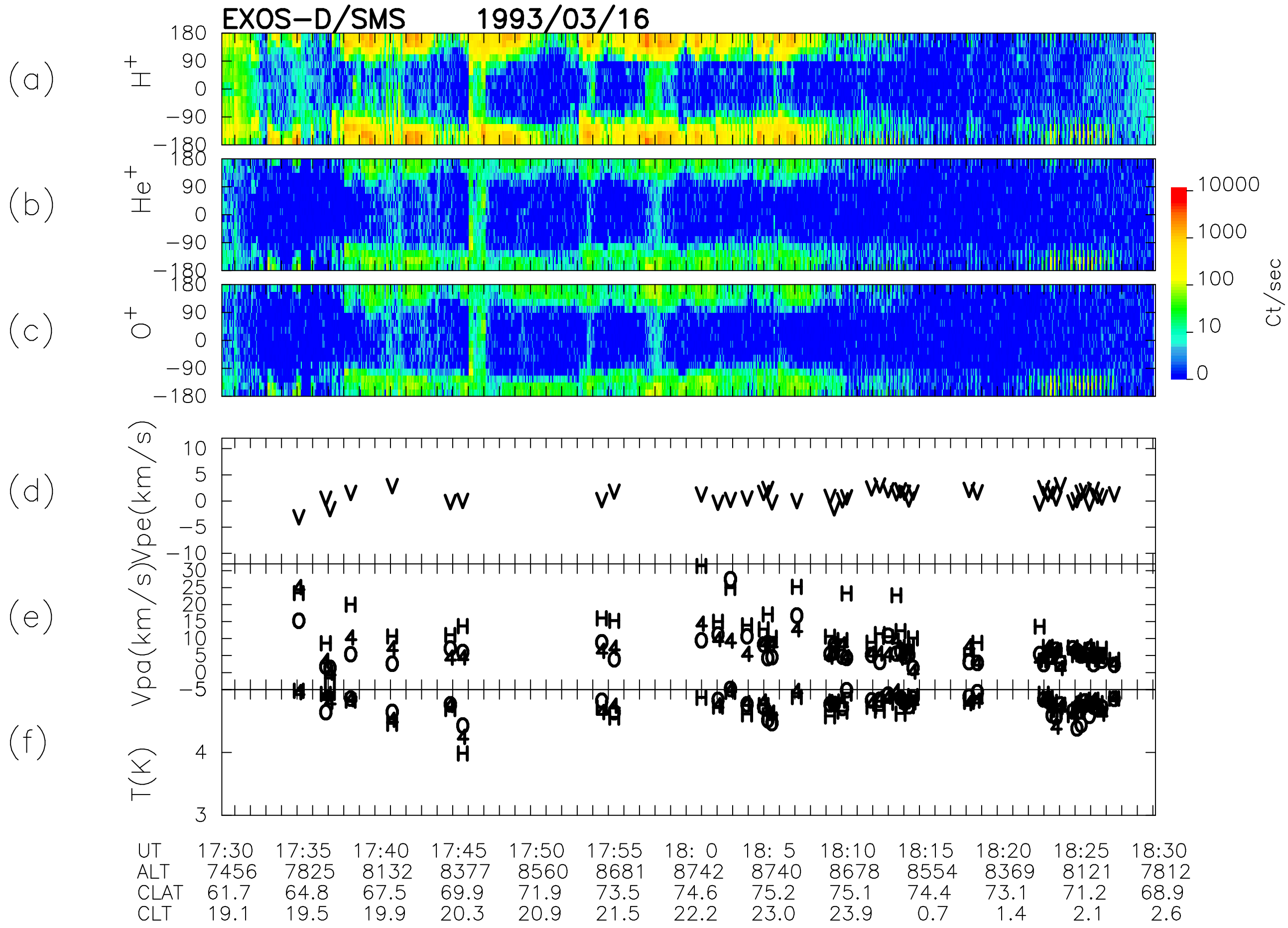
EXOS-D/SMS 1993/03/16
(a)
(b)
(c)
(d)
(e)
(f)
H+
He+
O+
Vpe(km/s)
Vpa(km/s)
T(K)
Ct/sec
10000
1000
100
10
0
UT 17:30 17:35 17:40 17:45 17:50 17:55 18: 0 18: 5 18:10 18:15 18:20 18:25 18:30
ALT 7456 7825 8132 8377 8560 8681 8742 8740 8678 8554 8369 8121 7812
CLAT 61.7 64.8 67.5 69.9 71.9 73.5 74.6 75.2 75.1 74.4 73.1 71.2 68.9
CLT 19.1 19.5 19.9 20.3 20.9 21.5 22.2 23.0 23.9 0.7 1.4 2.1 2.6

Figure 2.

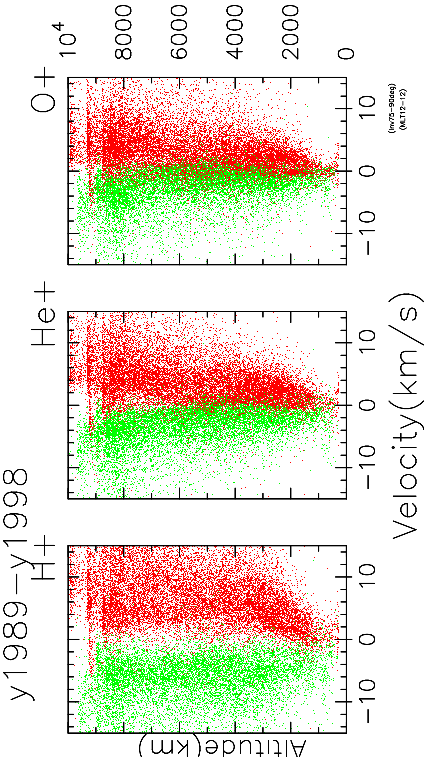
y1989−y1998
H+
He+
O+
Altitude(km)
Velocity(km/s)
10^4
8000
6000
4000
2000
0
−10
0
10

Figure 3.

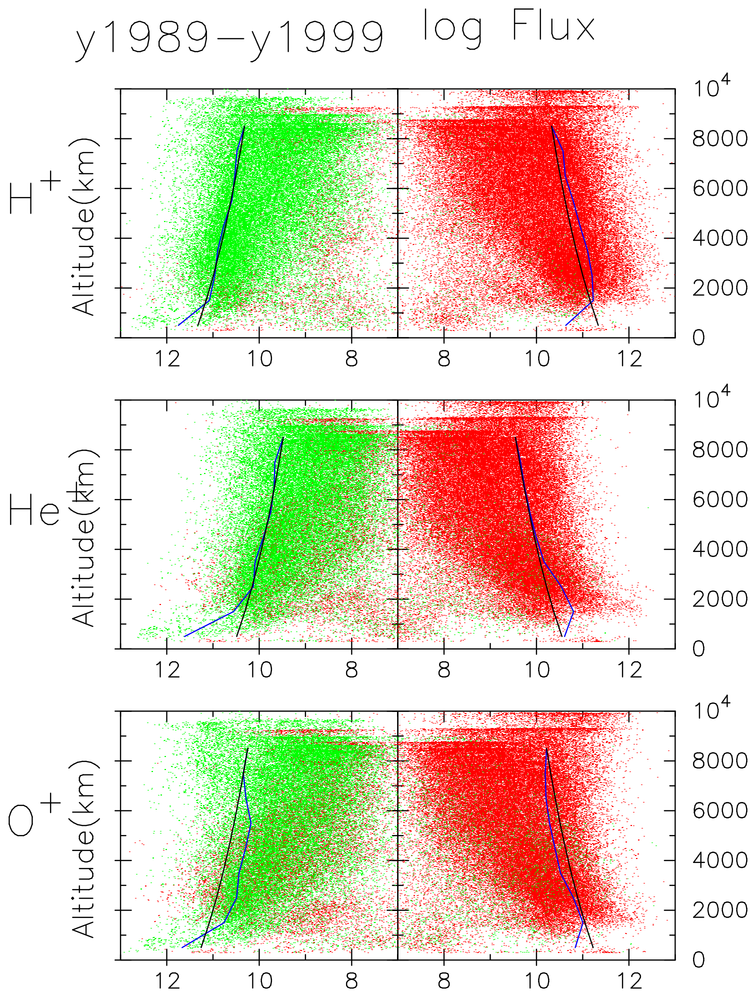
y1989–y1999 log Flux
H+
He+
O+
Altitude(km)
Altitude(km)
Altitude(km)
12
10
8
8
10
12
10^4
8000
6000
4000
2000
0

Figure 4.

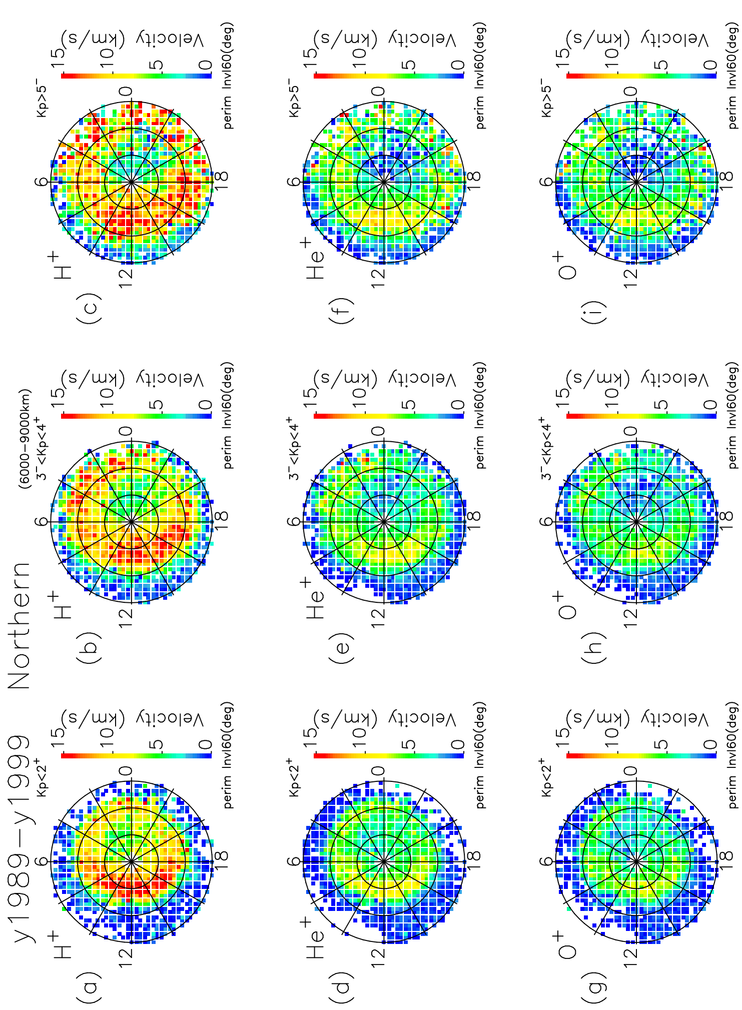
y1989−y1999
Northern
(6000−9000km)
(a) H+
(b) H+
(c) H+
(d) He+
(e) He+
(f) He+
(g) O+
(h) O+
(i) O+
Kp<2+
3−<Kp<4+
Kp>5−
Velocity (km/s)
perim Invl60(deg)

Figure 5.

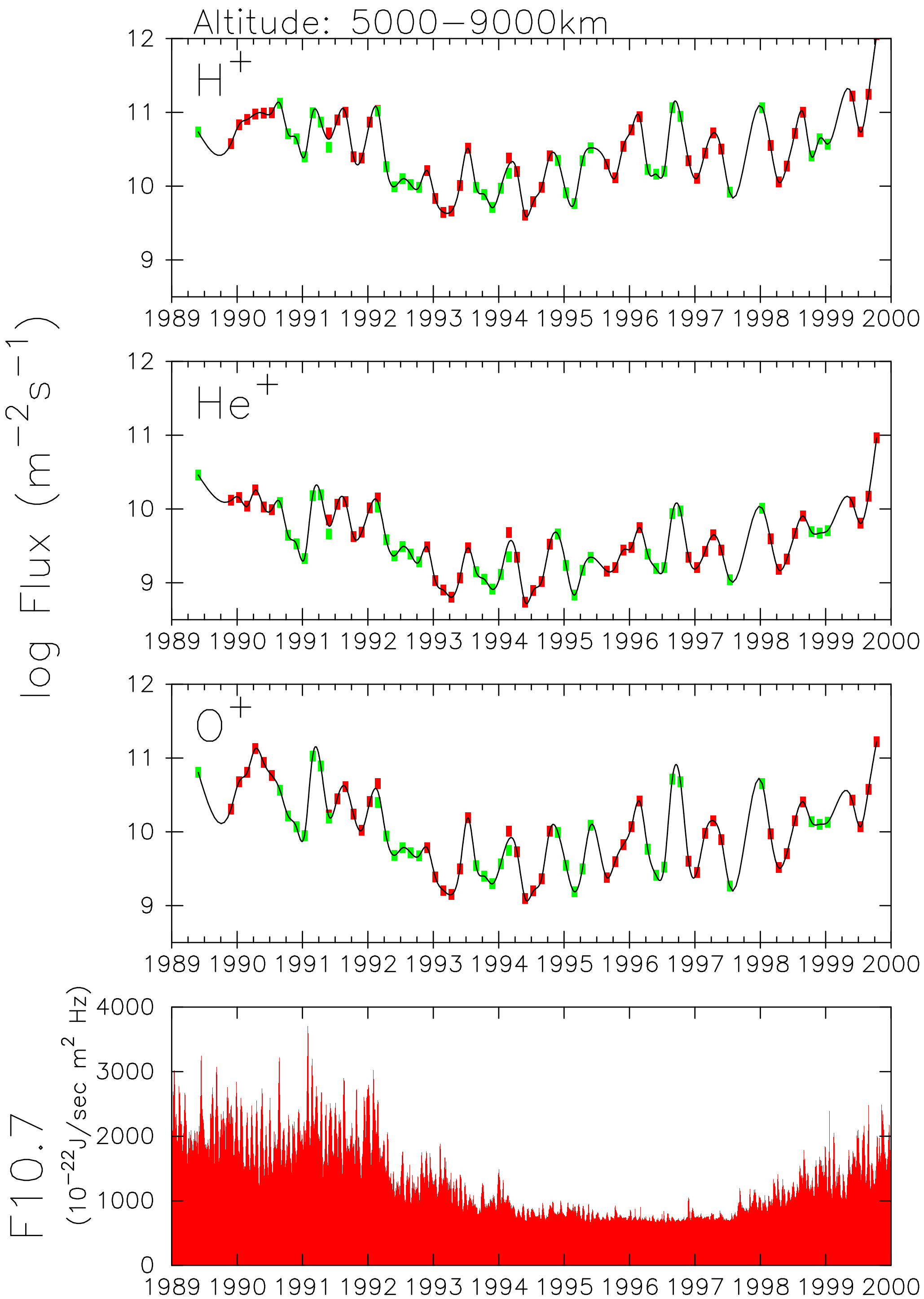
Altitude: 5000−9000km
H+
He+
O+
log Flux (m−2s−1)
F10.7
(10−22J/sec m2 Hz)
12
11
10
9
4000
3000
2000
1000
0
1989 1990 1991 1992 1993 1994 1995 1996 1997 1998 1999 2000

Figure 6.

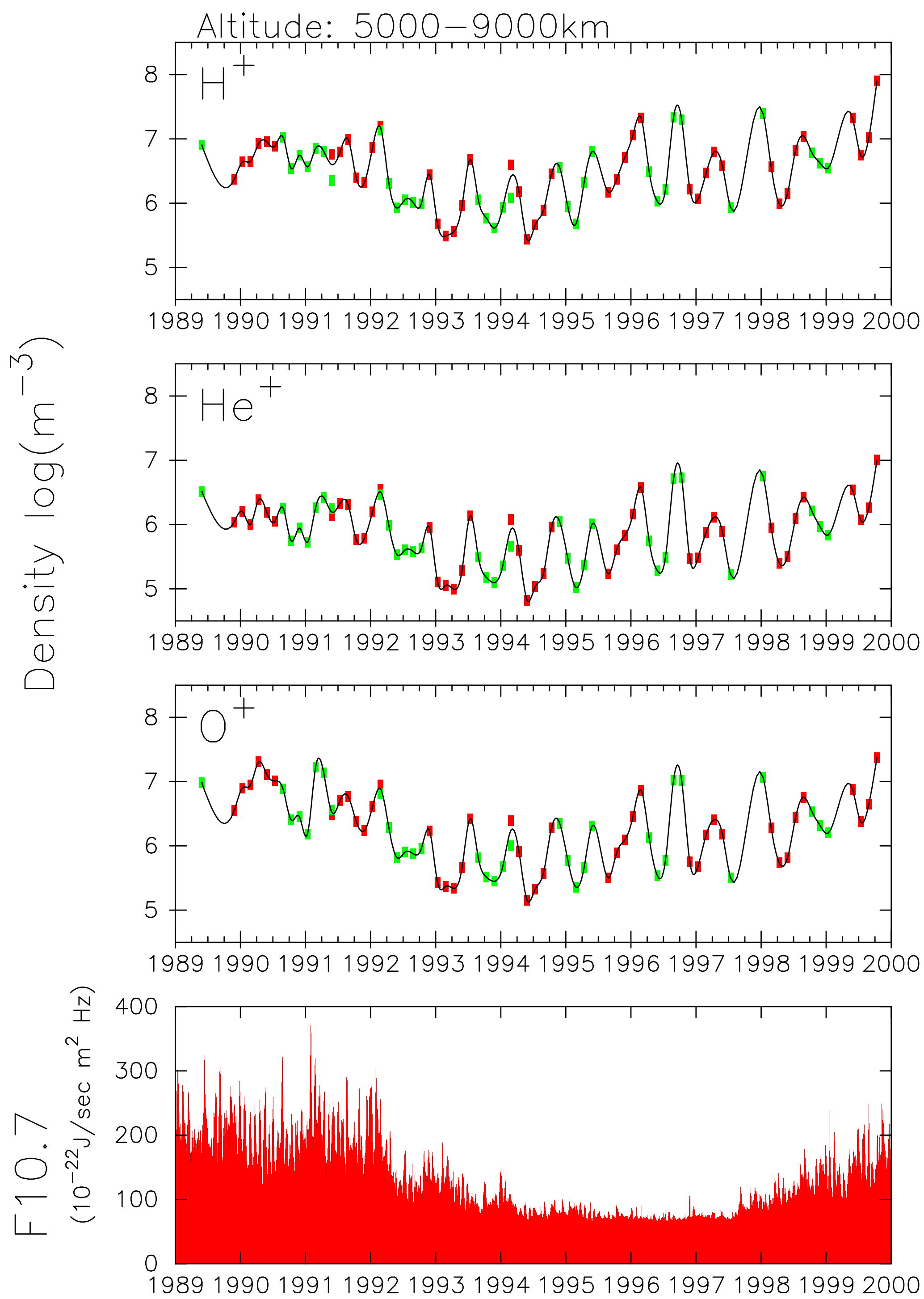
Altitude: 5000−9000km
H+
He+
O+
Density log(m−3)
F10.7
(10−22J/sec m2 Hz)
1989 1990 1991 1992 1993 1994 1995 1996 1997 1998 1999 2000

Figure 7.

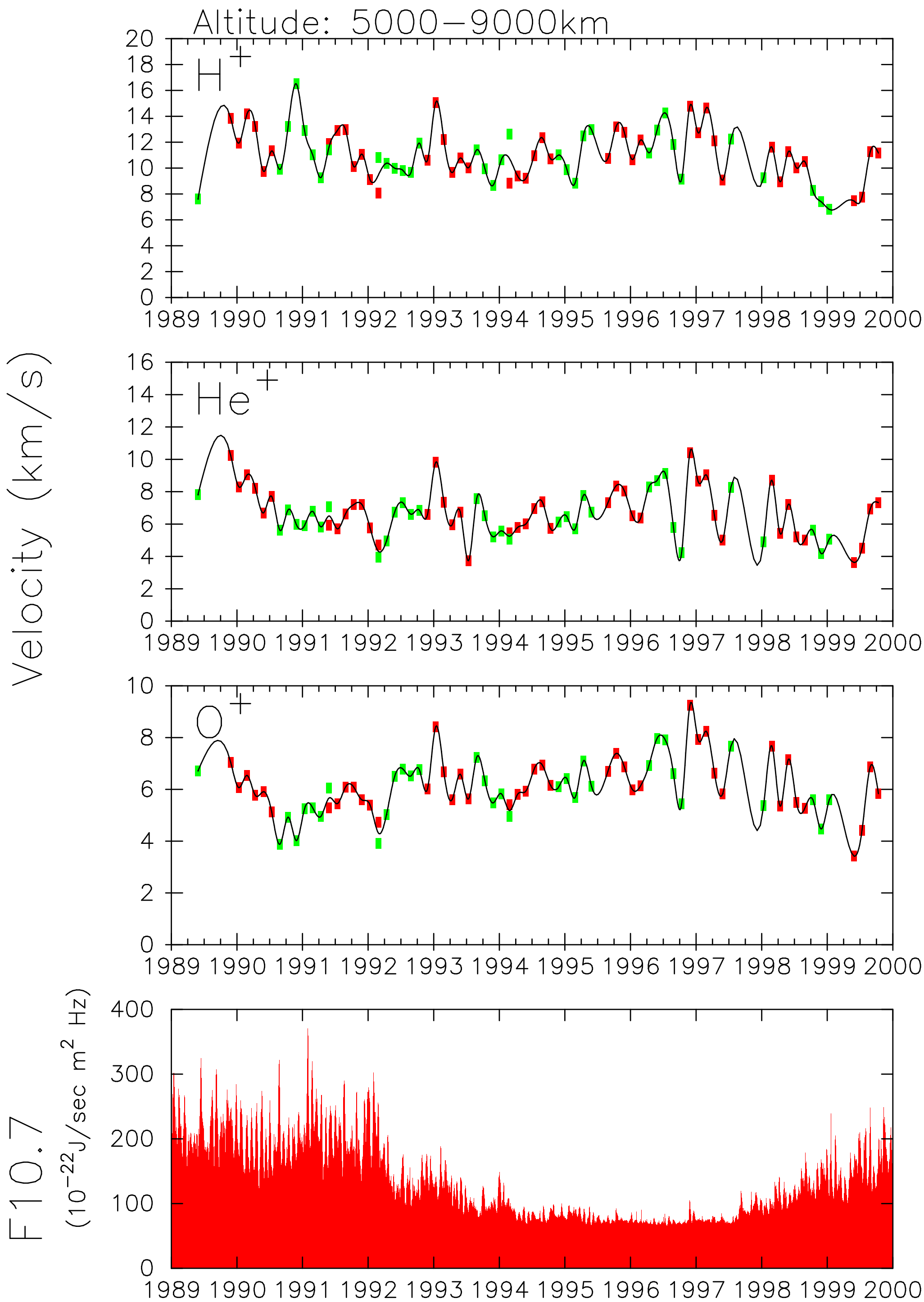
Altitude: 5000−9000km
H+
He+
O+
Velocity (km/s)
F10.7
(10−22J/sec m2 Hz)
1989 1990 1991 1992 1993 1994 1995 1996 1997 1998 1999 2000

Figure 8.

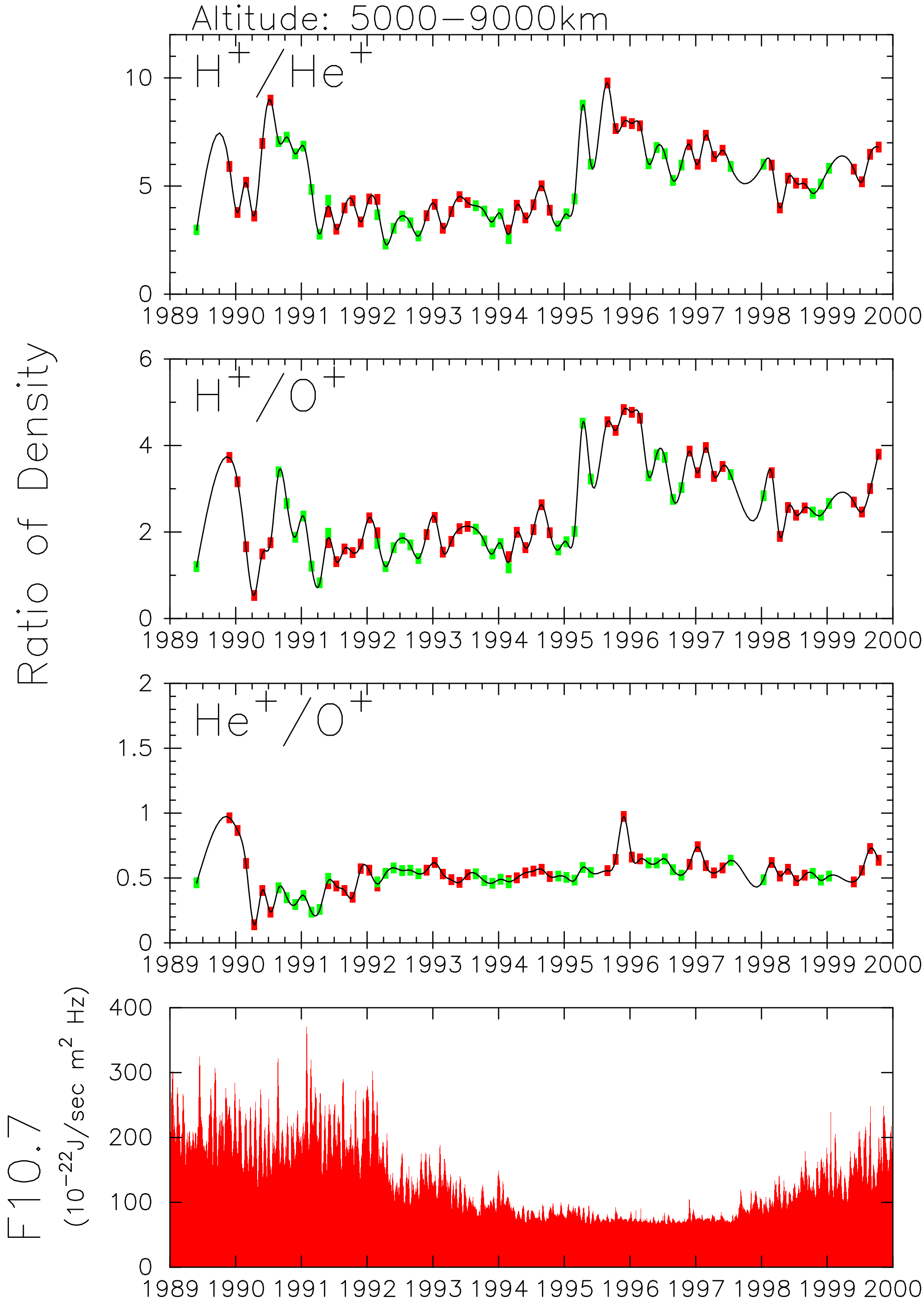
Altitude: 5000−9000km
H+/He+
H+/O+
He+/O+
Ratio of Density
F10.7
(10−22J/sec m2 Hz)
0
5
10
2
4
6
0.5
1
1.5
100
200
300
400
1989 1990 1991 1992 1993 1994 1995 1996 1997 1998 1999 2000

Figure 9.

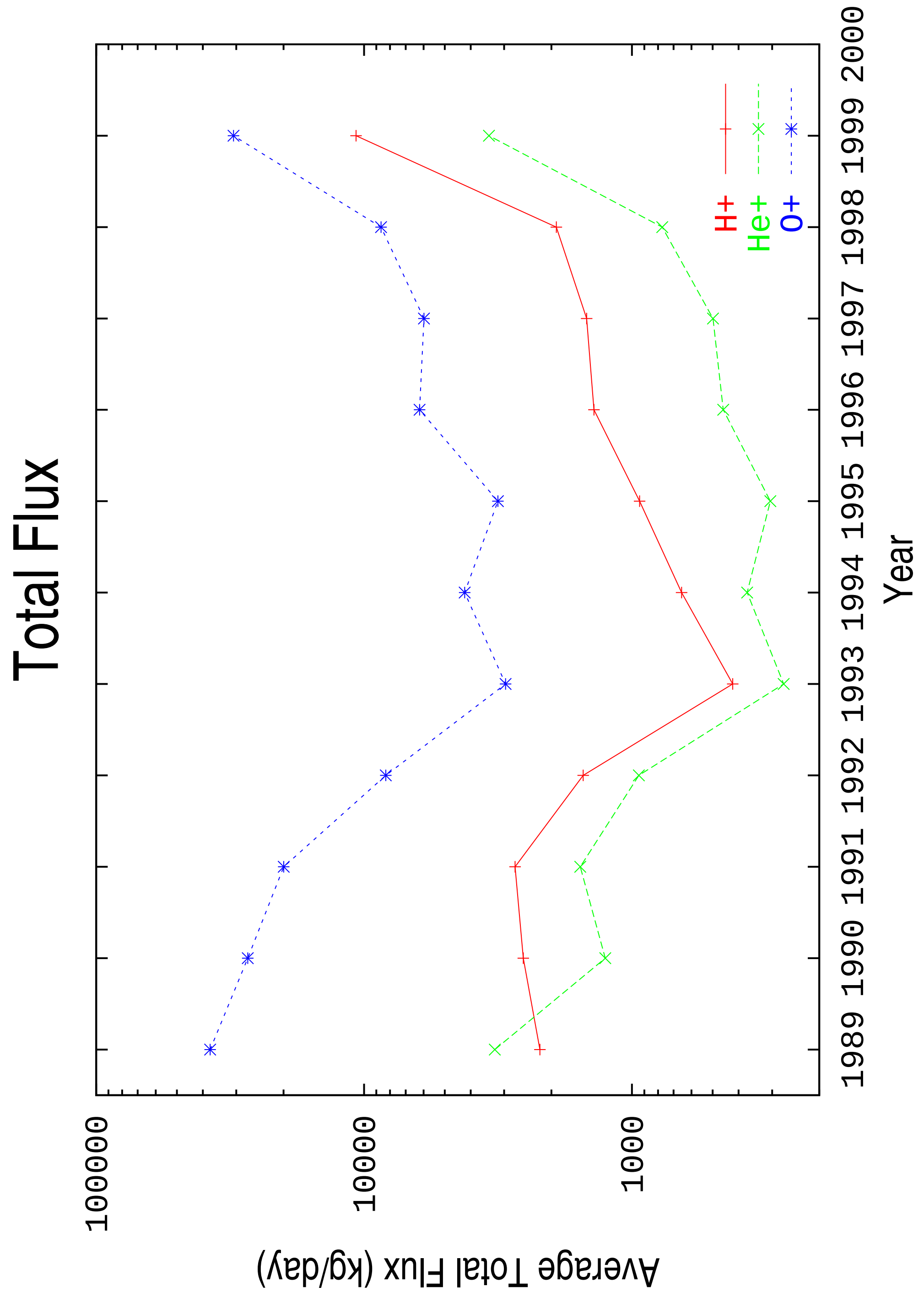
Total Flux
Average Total Flux (kg/day)
100000
10000
1000
Year
1989
1990
1991
1992
1993
1994
1995
1996
1997
1998
1999
2000
H+
He+
O+

Figure 10.